Glucose-1,6-bisphosphate, a key metabolic regulator, is synthesized by a distinct family of α-phosphohexomutases widely distributed in prokaryotes

Niels Neumann[1,2], Simon Friz[1,2] and Karl Forchhammer[1,2*]

[1] Interfaculty Institute of Microbiology and Infection Medicine, University of Tübingen, Auf der Morgenstelle 28, 72076 Tübingen, Germany

[2] Cluster of Excellence: EXC 2124: Controlling Microbes to Fight Infection, Tübingen, Germany

* For correspondence: karl.forchhammer@uni-tuebingen.de

Abstract

The reactions of α-D-phosphohexomutases (αPHM) are ubiquitous, key to primary metabolism and essential for several processes in all domains of life. The functionality of these enzymes relies on an initial auto-phosphorylation step which requires the presence of α-D-glucose-1,6-bisphosphate (Glc-1,6-BP). While well investigated in vertebrates, the origin of this activator compound in bacteria is unknown. Here we show that the Slr1334 protein from the unicellular cyanobacterium *Synechocysitis* sp. PCC 6803 is a Glc-1,6-BP-synthase. Biochemical analysis revealed that Slr1334 efficiently converts fructose-1,6-bisphosphate and α-D-glucose-1-phosphate/α-D-glucose-6-phosphate into Glc-1,6-BP and also catalyzes the reverse reaction. Phylogenetic analysis revealed that the *slr1334* product belongs to a primordial subfamily of αPHMs that is present especially in deeply branching bacteria and also includes human commensals and pathogens. Interestingly, the homologue of Slr1334 in the human gut bacterium *Bacteroides salyersiae* catalyzes the same reaction, suggesting a conserved and essential role for the members of this αPHM subfamily.

Key words:

Phosphoglucomutase, glucose-1,6-bisphosphate, fructose-1,6-bisphosphate, glycolysis, carbon metabolism

31 # Introduction

32 The α-D-phosphohexomutase (αPHM) superfamily is ubiquitous and found in all domains of
33 life. All known members of this superfamily catalyze a reversible intramolecular phosphoryl
34 transfer on their phosphosugar substrates. This reaction requires a bound metal ion (usually
35 Mg^{2+}) together with a conserved phosphorylated seryl residue in the active site and proceeds
36 via a bis-phosphorylated sugar intermediate [1]. While showing similar properties in structure
37 and reaction mechanism, these enzymes differ strongly in substrate specificity. Based on their
38 preferred substrate, the αPHMs are traditionally divided into four main groups: (1)
39 Phosphoglucomutases (PGM), (2) phosphoglucosamine mutases (PNGM), (3)
40 phosphoacetylglucosamine mutases (PAGM) and (4), the group of bifunctional
41 phosphoglucomutases/phosphomannomutases (PGM/PMM) [1]. The most recent expansion to
42 this classification has been the discovery of the mammalian phosphopentomutase (PGM2)
43 and Glucose-1,6-Bisphosphate-synthase (PGM2L1) [2, 3]. This classification, however, lacks a
44 more detailed subdivision in between the main groups and also does not take into account
45 αPHMs preferably catalyzing other reactions (e.g. straight phosphomannomutases) [3]. The
46 NCBI conserved domain database (CDD), instead, classifies the αPHM superfamily in 11
47 different subfamilies on a phylogenetic basis [4]. This phylogenetic model enables a more
48 detailed classification and includes several groups of bacterial and archaeal enzymes showing
49 typical αPHM properties but being only poorly characterized (**Table 1**).

CDD group name	CDD identifier	Proposed main function
PGM1	cd03085	Phosphoglucomutase
PGM2	cd05799	Phosphopentomutase (PGM2)/Glc-1,6-BP synthase (PGM2L1)
PGM3(PAGM)	cd03086	Phosphoacetylglucosamine mutase
PMM/PGM	cd03089	Bi-functional phosphomanno-/phosphoglucomutase
PGM like 1	cd03087	Unknown
PGM like 2	cd05800	Unknown
PGM like 3	cd05801	Phosphoglucomutase
PGM like 4	cd05803	Unknown
ManB	cd03088	Phosphomannomutase
GlmM	cd05802	Phosphoglucosamine mutase
Mpg1 transferase	cd05805	GDP-mannose-pyrophosphorylase

Table 1: Subfamilies in the αPHM superfamily with their identifier and proposed main function according to the NCBI conserved domain database (CDD)

50 The PGM (cd03085) from rabbit and human as well as the bacterial PGM (cd05801) from
51 *Salmonella typhimurium* and the bacterial bifunctional PMM/PGM (cd03089) from
52 *Pseudomonas aeruginosa* are among the best characterized αPHMs with available crystal
53 structures and detailed description of reaction mechanisms [5-9]. Catalyzing the interconversion
54 of α-D-glucose-1P (Glc-1P) and α-D-glucose-6P (Glc-6P) makes PGM a key enzyme in glycogen
55 metabolism, glycolysis and gluconeogenesis. During this reaction, a phosphoserine at the
56 active site of PGM donates the phosphoryl group to the substrate Glc-6P or Glc-1P resulting
57 in the synthesis of the transient intermediate α-D-glucose-1,6-bisphosphate (Glc-1,6-BP).
58 After a reorientation in the catalytic center, the intermediate product re-phosphorylates the
59 active site serine yielding Glc-1P or Glc-6P, respectively. Glc-1,6-BP itself acts as an essential
60 activator of PGM by providing an initial phosphorylation of the active site and was first
61 discovered by Leloir, Trucco [10] in yeast extract [11]. While Glc-1,6-BP is not a free metabolite in
62 any metabolic pathway, it is known to be a potent regulator of several enzymes in central
63 carbon metabolism in eukaryotes: in addition to PGMs and other αPHMs, it was shown to
64 regulate hexokinases, 6-phosphogluconate dehydrogenase, phosphofructokinase and
65 pyruvate kinase [12]. In mammalian tissues the synthesis of Glc-1,6-BP is catalyzed by the
66 PGM2L1 enzyme, a member of the cd05799 subfamily, utilizing 1,3-bisphosphoglyceric acid
67 (1,3-BPG) as phosphoryl donor for Glc-1P [3]. In contrast, despite its essential role in the activity
68 of prokaryotic PGM, the function of Glc-1,6-BP in prokaryotes has been overlooked and its
69 origin remains obscure as no enzyme producing free Glc-1,6-BP has been identified so far [13].
70 The unicellular cyanobacterium *Synechocystis* sp. PCC 6803 (hereafter *Synechocystis*) has two
71 enzymes that are encoded by the genes *sll0726* and *slr1334* and annotated as PGM-like [4].
72 While Sll0726 exhibits typical properties of PGMs [14-16], little is known about Slr1334. The only
73 study addressing this issue reported that purified *Synechocystis* Sll0726 has about a tenfold
74 higher activity *in vitro* than Slr1334 and that a *sll0726* knockout mutant only shows around
75 3 % PGM activity compared to the wildtype [17]. Despite its low contribution to over-all PGM
76 activity, the Slr1334 product appeared to be essential as it was not possible to acquire fully
77 segregated knockout mutants of the *slr1334* gene, which raised the question of the role of
78 Slr1334 in *Synechocystis*.
79
80 In this work we show that Slr1334 has a phosphotransferase activity catalyzing the production
81 of free Glc-1,6-BP from Glc-1P/Glc-6P and Fructose-1,6-bisphosphate (Frc-1,6-BP). Thereby,

82 Slr1334 is responsible for the formation of the key activator of PGM, Glc-1,6-BP, making it a
83 major regulator in glycolysis and other carbon pathways. Our finding makes Slr1334 the first
84 bacterial enzyme specific for the production of free Glc-1,6-BP. Importantly, we show that the
85 homologue of Slr1334 in the human gut bacterium *Bacteroides salyersiae* catalyzes the same
86 reaction.
87
88

89 # Results

90 **Classification of the two PGM isoenzymes from *Synechocystis***

91 *Synechocystis* possesses two genes annotated as PGMs, the genes *sll0726* and *slr1334*. In
92 order to classify them within the αPHM superfamily, we performed a phylogenetic analysis by
93 multi-level alignment of all αPHM subfamilies that are considered PGM or "PGM_like". For
94 this, we collected the entry sequences from the NCBI Conserved Domains Database (CDD) [4]
95 and retrieved further sequences by performing BLAST searches in the NCBI RefSeq_protein
96 database. To focus on glucose-specific αPHMs, the groups of enzymes specific for other sugars
97 like PMMs, PNGM and PAGMs (cd03086 cd03088, cd05802, cd05805) were omitted from the
98 analysis (**Fig. 1**). Slr1334 is part of the cd05800 (PGM like 2) subfamily present in many
99 bacterial groups. In agreement with the CDD, our phylogenetic analysis shows that this
100 subfamily forms a distinct cluster of PGMs which clearly separates from other PGM and PGM
101 like enzymes. The Sll0726 PGM, by contrast, is a member of the cd05801 subfamily, to which
102 the well characterized PGM from *S. typhimurium* belongs.
103
104
105
106
107

108

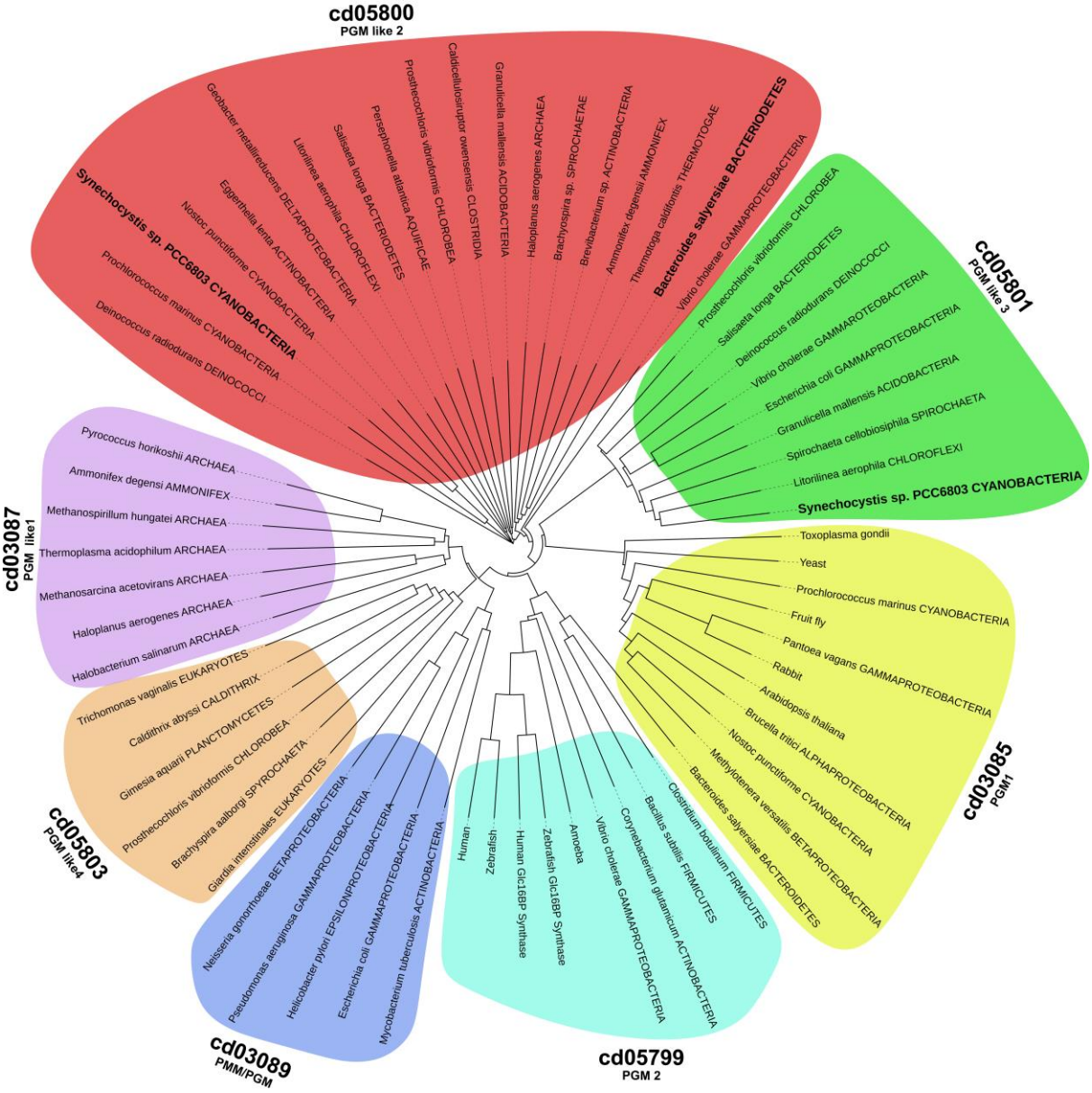

Figure 1: **Phylogenetic tree of the αPHM subfamilies that are considered to be "PGM-like" according to CDD**

The tree was built on the taxonomy based on the protein sequences present in the NCBI RefSeq_protein database. The CDD subfamilies cd03086, cd03088, cd05802 and cd05805, which are known to catalyze distinct reactions, were omitted from the analysis. The organisms investigated in this study are highlighted in bold letters.

109

110

111 **Slr1334 shows low PGM activity compared to Sll0726 but behaves differently in presence**
112 **of Fructose-1,6-BP**

113 To gain deeper insights into the role of the enigmatic Slr1334, we overexpressed Sll0726 along
114 with Slr1334 in *Escherichia coli* and assessed the PGM enzymatic activity of the purified
115 proteins by measuring the interconversion of Glc-1-P to Glc-6-P in an assay that couples Glc-
116 6-P formation to its subsequent oxidation using Glucose-6-phosphate-dehydrogenase
117 (G6PDH) and $NADP^+$. We could show that Slr1334 only displays about 5% of catalytic efficiency
118 compared to Sll0726 when both PGMs were tested with saturating amounts of the activator
119 Glc-1,6-BP (60 µM) (**Fig. 2, Table 2. See also Fig. 3**). Interestingly, the PGM activity of both
120 enzymes was also measurable without addition of Glc-1,6-BP, which is considered to be an
121 essential activator. However, in the absence of Glc-1,6-BP, the catalytic efficiency was about
122 70 times lower due to a significantly increased Michaelis-Menten constant (K_m) for Sll0726 and
123 Slr1334 alike.
124 Fructose-1,6- bisphosphate is an endogenous intermediate of the glycolytic pathway and is
125 known to be an inhibitor of PGM most likely by competing with the reaction intermediate Glc-
126 1,6-BP [18, 19]. In a preliminary experiment we tested the effect of different concentrations of
127 Frc-1,6-BP on Sll0726 and observed major inhibition already at concentrations of 100 µM (data
128 not shown). When testing PGM activity by replacing 60 µM Glc-1,6-BP with 100 µM Frc-1,6-
129 BP, we detected a decrease in catalytic efficiency to 19 % as a consequence of a strongly
130 increased K_m (**Fig. 2, Table 2**). Strikingly, however, for Slr1334 we detected a different effect:
131 while the catalytic rate constant (k_{cat}) decreased by about 2-fold, we measured an
132 approximately 100-fold reduced K_m resulting in a 50 times increased catalytic efficiency. This
133 raised the question of how Frc-1,6-BP affected the PGM-activity of Slr1334. We speculated
134 that Frc-1,6-BP might either function as a direct activator similar to Glc-1,6-BP or be required
135 for the synthesis of the activating compound Glc-1,6-BP during the reaction of Slr1334. As we
136 will show below, the activating compound turned out to be Glc-1,6-BP and not Frc-1,6-BP.
137
138
139
140
141
142

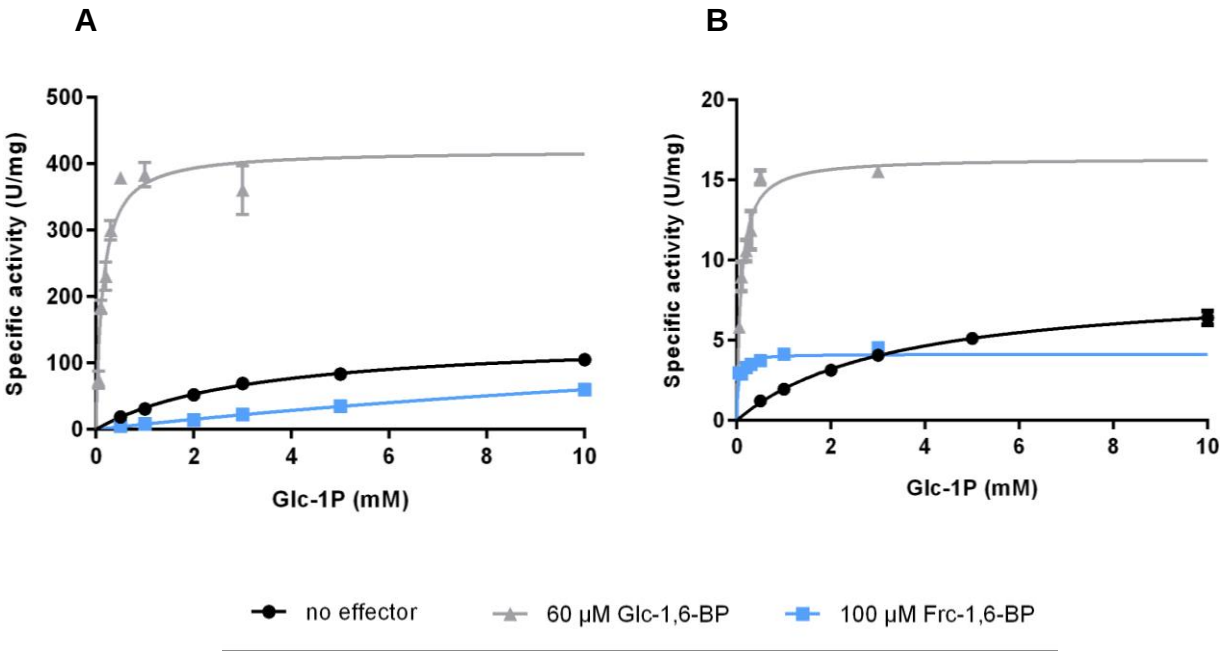

Figure 2: Slr1334 shows lower PGM activity then Sll0726 and behaves differently in presence of Frc-1,6-BP

Shown are the Michaelis-Menten kinetics of Sll0726 (A) and Slr1334 (B): in black, without addition of effectors; in light grey in the presence of 60 µM Glc-1,6-BP; in blue, in the presence of 100 µM Frc-1,6-BP. Three replicates were measured for each data-point. Error bars represent the SD.

Effector	Sll0726			Slr1334			
	K_m (mM)	k_{cat} (s^{-1})	k_{cat}/K_m ($M^{-1}s^{-1}$)	K_m (mM)	k_{cat} (s^{-1})	k_{cat}/K_m ($M^{-1}s^{-1}$)	Catalytic efficiency ratio (%) (Slr1334/Sll0726)
No effector	3.27 ± 0.21	138 ± 3.7	42.2 *10^3	3.31 ± 0.14	7.5 ± 0.1	2.3 * 10^3	**5.5**
Glc-1,6-BP	0.19 ± 0.04	415 ± 30.6	3038.9 * 10^3	0.09 ± 0.02	14.4 ± 0.7	158.1 * 10^3	**5.2**
Frc-1,6-BP	26.86 ± 3.35	218 ± 21.3	8.1 * 10^3	0.03 ± 0.01	3.6 ± 0.2	117.5 * 10^3	**1450**

Table 2: Kinetic parameters of Sll0726 and Slr1334 with different effector molecules
K_m and K_{cat} values are means of triplicates with ± SD. Catalytic efficiency ratio is given in percentage and was calculated by the ratio of K_{cat}/K_m of Slr1334 and Sll0726.

168 **Slr1334 forms a product out of Frc-1,6-BP and Glc-1P/Glc-6P that strongly activates Sll0726**

169 To determine the amount of Glc-1,6-BP needed to achieve activation of Sll0726 at 1 mM Glc-
170 1P we first tested enzymatic activity of Sll0726 at different Glc-1,6-BP concentrations.
171 Maximum activation was achieved at Glc-1,6-BP concentrations between 30 and 60 µM
172 resulting in a 5-fold increased activity as compared to the zero Glc-1,6-BP reaction (**Fig. 3**).
173 Next, we incubated Slr1334 with the phosphorylated sugars Frc-1,6-BP, Glc-1P and Glc-6P (1
174 mM each) in different combinations and subsequently tested whether Sll0726 could be
175 activated by the corresponding reaction products (**Fig. 3**). As negative control, Frc-1,6-BP and
176 Glc-1P were allowed to react without any enzyme or with Sll0726 instead of Slr1334. After
177 running the Slr1334 reaction for 1.5 h, the reaction was stopped by heat inactivation and the
178 supernatant was added in a dilution of 1:10 to the reaction mixture of the Sll0726 assay, which
179 was then started by adding 1 mM Glc-1P. Only after adding the supernatant of the Slr1334
180 reaction containing Frc-1,6-BP and Glc-1P (or Glc-6P) as substrates, the velocity of the Sll0726
181 reaction was increased by 5-fold in comparison to the control reaction at zero Glc-1,6-BP (**Fig.**
182 **3**). When the Sll0726 test reaction was performed with the supernatant of the Sll0726 control
183 reaction or the reaction products of Slr1334 using Frc-1,6-BP as sole substrate, the enzyme
184 velocity was lower than the zero Glc-1,6-BP reaction. This reduction can be explained by the
185 inhibitory effect of Frc-1,6-BP on Sll0726, as exemplified by the "no enzyme control" reaction
186 (**Fig. 3**).
187
188 In addition to Frc-1,6-BP, we also tested whether Slr1334 can utilize 1,3-BPG instead of Frc-
189 1,6-BP for Glc-1,6-BP formation as described for the mammalian PGM2L1. Since 1,3-BPG is not
190 commercially available, we established an assay whereby we continuously produced 1,3-BPG
191 by a phosphoglycerate kinase (PGK) reaction using a His-tagged purified PGK in combination
192 with 1 mM 3PG and 1 mM ATP (see methods part). This reaction was directly coupled to the
193 reaction of Slr1334 with Glc-1P or Glc-6P or no substrate. As a control the same reaction was
194 performed with Sll0726 instead of Slr1334. To test the possible formation of Glc-1,6-BP, the
195 supernatants of these reactions were added to the Sll0726 reaction before performing the
196 enzymatic assay as described above.
197 We detected an increase in Sll0726 activity by approx. 2.5-fold compared to the zero Glc-1,6-
198 BP reaction when the supernatant of the Slr1334 reaction contained 1,3-BPG and either Glc-
199 1P or Glc-6P. No increase in activity was detected when the supernatant solely contained 1,3-

200 BPG. The supernatant of the control reaction with Sll0726 instead of Slr1334 resulted in no
201 marked change in activity.
202 By comparing the activation of Sll0726 by the Slr1334 reaction products to the activation of
203 Sll0726 at different concentration of Glc-1,6-BP we could estimate the efficiency of Glc-1,6-BP
204 formation from Frc-1,6-BP or 1,3-BPG. With Frc-1,6-BP as substrate for the Slr1334 reaction,
205 a maximum activation of Sll0726 was achieved, which corresponded to activation of Sll0726
206 with concentrations of Glc-1,6-BP between 30 and 60 µM (**Fig. 3**). When 1,3-BPG was used as
207 substrate as described above, the increase in Sll0726 activity corresponded to Glc-1,6-BP
208 concentrations between 1 and 5 µM. From this experiment we conclude that i) Slr1334 forms
209 a product out of Glc-1P/Glc-6P and either Frc-1,6-BP or 1,3-BPG that is able to activate Sll0726
210 similar to defined amounts of Glc-1,6-BP; ii) when normalizing the Sll0726 activation to Glc-
211 1,6-BP concentrations, the reaction product of Slr1334 using Frc-1,6-BP as phosphorylating
212 sugar is 10-fold more effective in activating Sll0726 than using 1,3-BPG.
213
214
215
216
217
218
219
220
221
222

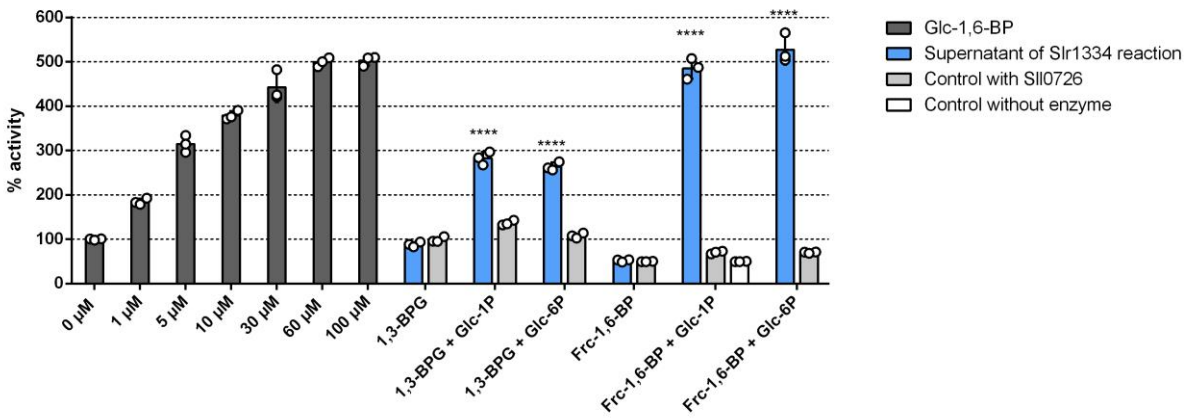

223 **Figure 3: Slr1334 produces a compound out of Frc-1,6-BP that strongly activates Sll0726**

224 Shown is the Sll0726 activity: in dark grey, at different Glc-1,6-BP concentrations; in blue,
225 after addition of the supernatant of the Slr1334 reaction; in light grey, after addition of the
226 supernatant of the Sll0726 reaction as a control; in white, after addition of the sole
227 phosphosugars without enzyme as further control. The different combinations of
228 substrates used for the Slr1334 reaction and controls are indicated on the X-axis. Values
229 represent relative activity compared to the Sll0726 reaction with 0 µM Glc-1,6-BP, which
was considered 100%. Three biological replicates were measured for each datapoint. Error
bars represent the SD; asterisks represent the statistical significance.

230

231

232 **The product of the Slr1334 reaction is not degradable by the Frc-1,6-BP-aldolase**

233 To confirm that the activating compound formed from Glc-1P/Glc-6P and Frc-1,6-BP through
234 the Slr1334 reaction is in fact Glc-1,6-BP, we analyzed the reaction product via liquid
235 chromatography-mass spectrometry (LC/MS). Therefore, we incubated Slr1334 together with
236 500 µM Frc-1,6-BP and 1 mM Glc-1P for 1.5 h. As a control, the same substrates were
237 incubated without enzyme. Since LC/MS analysis does not allow discriminating Glc-1,6-BP
238 from Frc-1,6-BP, we performed an additional reaction step to specifically degrade Frc-1,6-BP.
239 Therefore, after heat inactivation, the reaction mixture was incubated with Frc-1,6-BP-
240 aldolase (Fba) and glycerol-3-phosphate-dehydrogenase (GPDH) as well as 1 mM NADH: Fba
241 specifically cleaves Frc-1,6-BP into dihydroxyacetone phosphate (DHAP) and glyceraldehyde-
242 3P while Glc-1,6-BP is unaffected. GPDH subsequently forms glycerol-3-phosphate (glycerol-
243 3P) and NAD^+ out of DHAP and NADH. This is necessary to enable full degradation of Frc-1,6-
244 BP.
245 After this treatment, LC/MS analysis revealed that a compound with a mass corresponding to
246 either Glc-1,6-BP or Frc-1,6-BP was present in the Slr1334 reaction while this mass was not
247 detectable in the control reaction where no Slr1334 was present (**Fig. 4**). This indicates that
248 Frc-1,6-BP in the control reaction was completely degraded in the subsequent reaction by Fba
249 as expected, while Frc-1,6-BP in the Slr1334 reaction was metabolized into a molecule of the
250 same mass that was not degraded by Fba. This is precisely what is expected when Glc-1,6-BP
251 is produced form Frc-1,6-BP turn-over. Furthermore, the reaction products from the coupled
252 GPDH reaction, NAD+ and glycerol-3P were more abundant in the control reaction without
253 Slr1334 as compared to the reaction with Slr1334. This indicated that more Frc-1,6-BP was
254 degraded out of the control reaction than out of the reaction containing Slr1334 due to partial
255 conversion of Frc-1,6-BP into Glc-1,6-BP by Slr1334 (**Fig. 4**). Altogether, this experiment
256 strongly indicated that in the presence of Slr1334, Frc-1,6-BP was partially utilized to form Glc-
257 1,6-BP. The fact that only a part of Frc-1,6-BP was consumed could be either due to a too short
258 reaction time or because the reaction reached an equilibrium state.
259
260
261
262
263

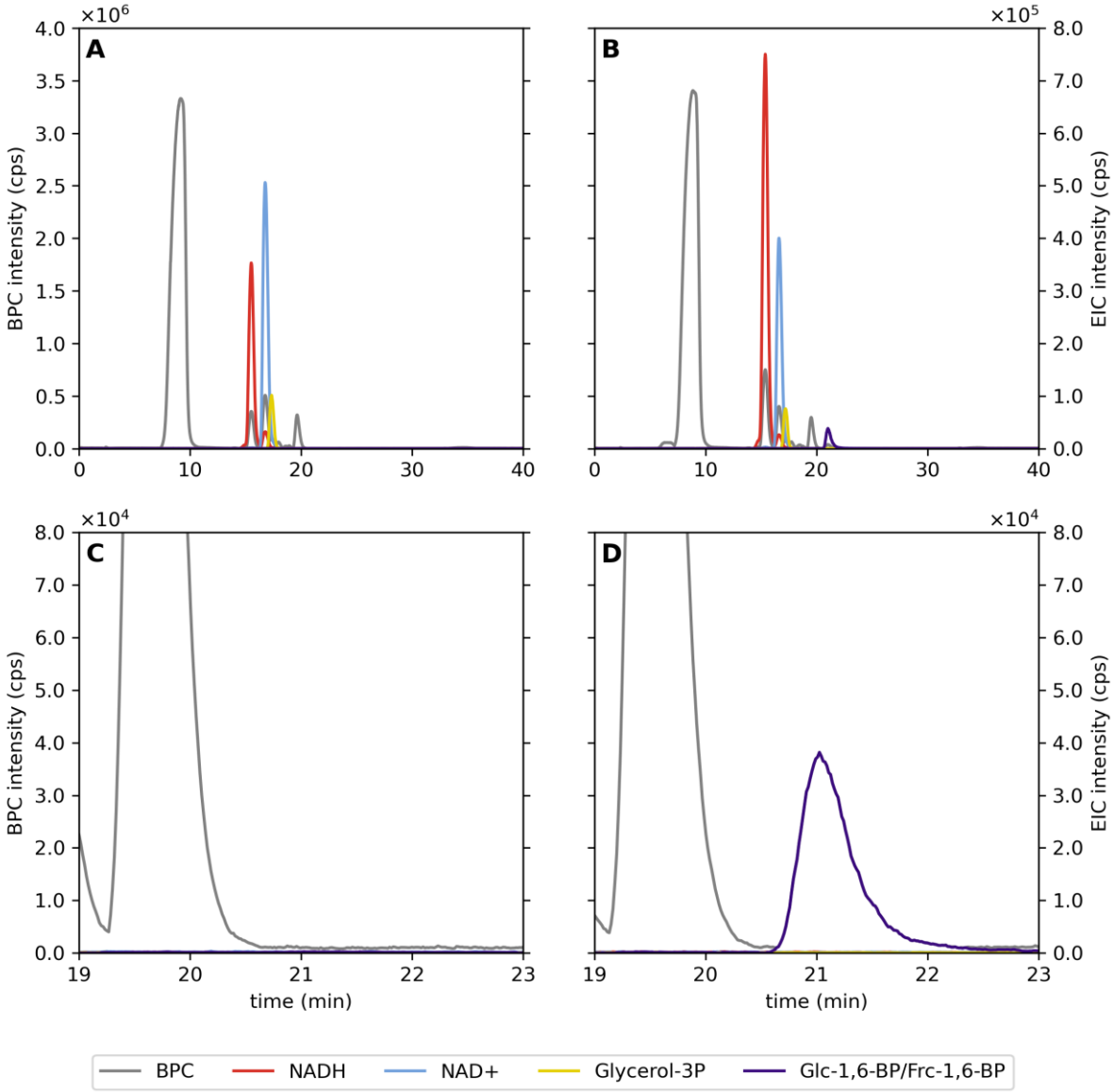

Figure 4: LC-MS analysis reveals that Slr1334 metabolizes Frc-1,6-BP into a molecule of identical mass that is not degraded by Frc-1,6-BP-aldolase

Analysis of the products of the reaction without (A) and with Slr1334 (B) via LC/MS. Shown are the base peak chromatograms (BPC) in the mass range $(M\text{-}H)^-$ m/z = 79–1,601 (grey) and the extracted ion chromatograms (EIC) based on the exact masses of NAD+ $(M\text{-}H)^-$= 662.101 m/z (light blue), NADH $(M\text{-}H)^-$= 664.117 m/z (red), Glycerol 3-P $(M\text{-}H)^-$= 171.006 m/z (yellow), Glc-1,6-BP/Frc-1,6-BP $(M\text{-}H)^-$= 338.988 m/z (purple). The presence of the NAD+ (blue) and Glycerol-3P (yellow) peaks in (B) shows that Frc-1,6-BP was not fully metabolized into Glc-1,6-BP. Magnification and adjustment of the graphs in (A) and (B) is clear evidence of the absence (C) or formation (D) of Glc-1,6-BP.

296 **Slr1334 keeps Frc-1,6-BP and Glc-1,6-BP in an equilibrium**

297 For investigating whether the formation of Glc-1,6-BP out of Glc-1P/Glc-6P and Frc-1,6-BP is
298 an equilibrium reaction, we performed an enzymatic assay to determine the amount of the
299 remaining Frc-1,6-BP. Therefore, Slr1334 was incubated with 500 µM of Frc-1,6-BP and 1 mM
300 Glc-1P for 1.5 h. As controls, the same assays were performed with Sll0726 or without any
301 enzyme. After the reaction was stopped by heat inactivation, the supernatant was used to run
302 the coupled Fba/GPDH assay in a dilution of 1:10, which would correspond to a final
303 concentration of 50 µM Frc-1,6-BP if no Frc-1,6-BP was consumed. As further controls,
304 standards of 50 µM and 25 µM Frc-1,6-BP were used in the Fba/GPDH assay. This experiment
305 showed that the concentration of Frc-1,6-BP decreased by about 50 % when in the first
306 reaction Slr1334 was present, while apparently no Frc-1,6-BP was utilized in the control
307 reactions (**Fig. 5**). This result agreed with the assumption that the reaction reaches an
308 equilibrium at 50 % product formation, either because of the reversibility of the reaction or
309 product inhibition.
310
311
312
313
314
315
316
317
318
319
320
321

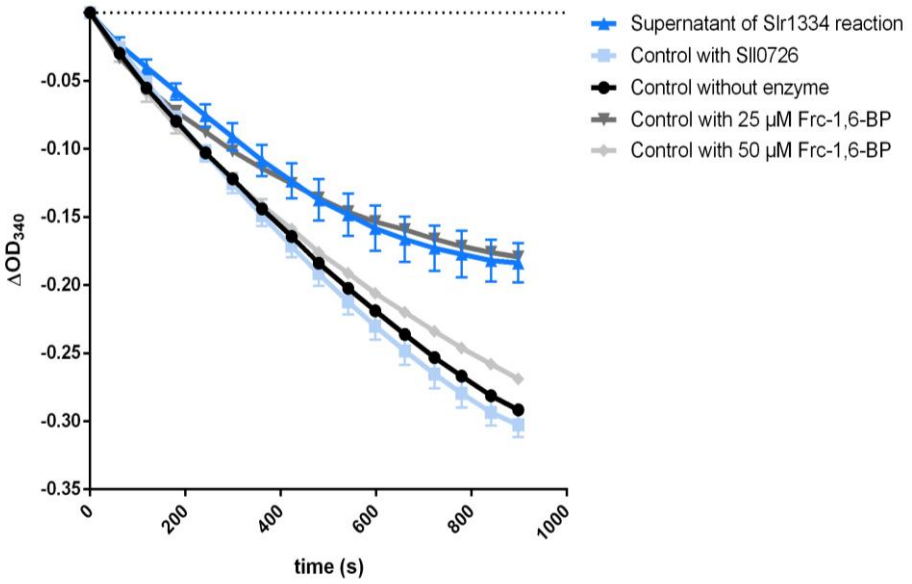

322 **Figure 5: Slr1334 produces Glc-1,6-BP out of Frc-1,6-BP in an equilibrium reaction**

323 Shown is the Frc-1,6-BP-aldolase activity: in dark blue, after addition of the supernatant of
324 the Slr1334 reaction; in light blue, after addition of the supernatant of the Sll0726 reaction
as a control; in black, after addition of the supernatant without any enzyme. In dark grey
325 and light grey, the aldolase activity measured at Frc-1,6-BP concentrations of 25 µM and
326 50 µM, respectively, as further control.
Frc-1,6-BP was used at concentrations of 500 µM in the Slr1334 reaction and respective
327 control reactions. Therefore, its final concentration in the Sll0726 assay after 1:10 dilution
was expected to be 50 µM assuming no consumption of Frc-1,6-BP in the Slr1334 reaction.

328 **The Slr1334 reaction is reversible**

329 To reveal whether Slr1334 can catalyze the proposed reverse reaction and synthesize Frc-1,6-
330 BP from Glc-1,6-BP and Fructose-1P (Frc-1P)/Fructose-6P (Frc-6P), formation of Frc-1,6-BP was
331 coupled to the Fba and GPDH reaction. For the assay, 50 µM Glc-1,6-BP was used and the
332 reaction was started by the addition of 5 mM Frc-6-P. As control reactions, *Synechocystis*
333 Sll0726 as well as PGM1 from rabbit were used. The results clearly showed that Slr1334 could
334 produce Frc-1,6-BP, resulting in measurable aldolase activity while the controls showed no
335 activity (**Fig. 6a**). Using this assay, we tried to determine the kinetic constants for the two
336 substrates Frc-6-P and Glc-1,6-BP. For Frc-6P, a K_m of 1 mM and a K_{cat} of 1.2 s^{-1} could be
337 determined (**Fig. 6b, Table 3**). By contrast, the affinity of Slr1334 for Glc-1,6-BP was so high
338 that, even at the lowest measurable substrate concentrations (2 µM), the reaction proceeded
339 with maximal velocity (**Fig. 6c**). Altogether these experiments unequivocally demonstrate that
340 Slr1334 is the first characterized bacterial Glc-1,6-BP synthase. In contrast to the eukaryotic
341 Glc-1,6-BP synthase, the prokaryotic enzyme uses Frc-1,6-BP as major phosphoryl donor for
342 Glc-1,6-BP production.
343
344
345
346
347
348
349
350
351
352
353
354
355
356
357
358
359

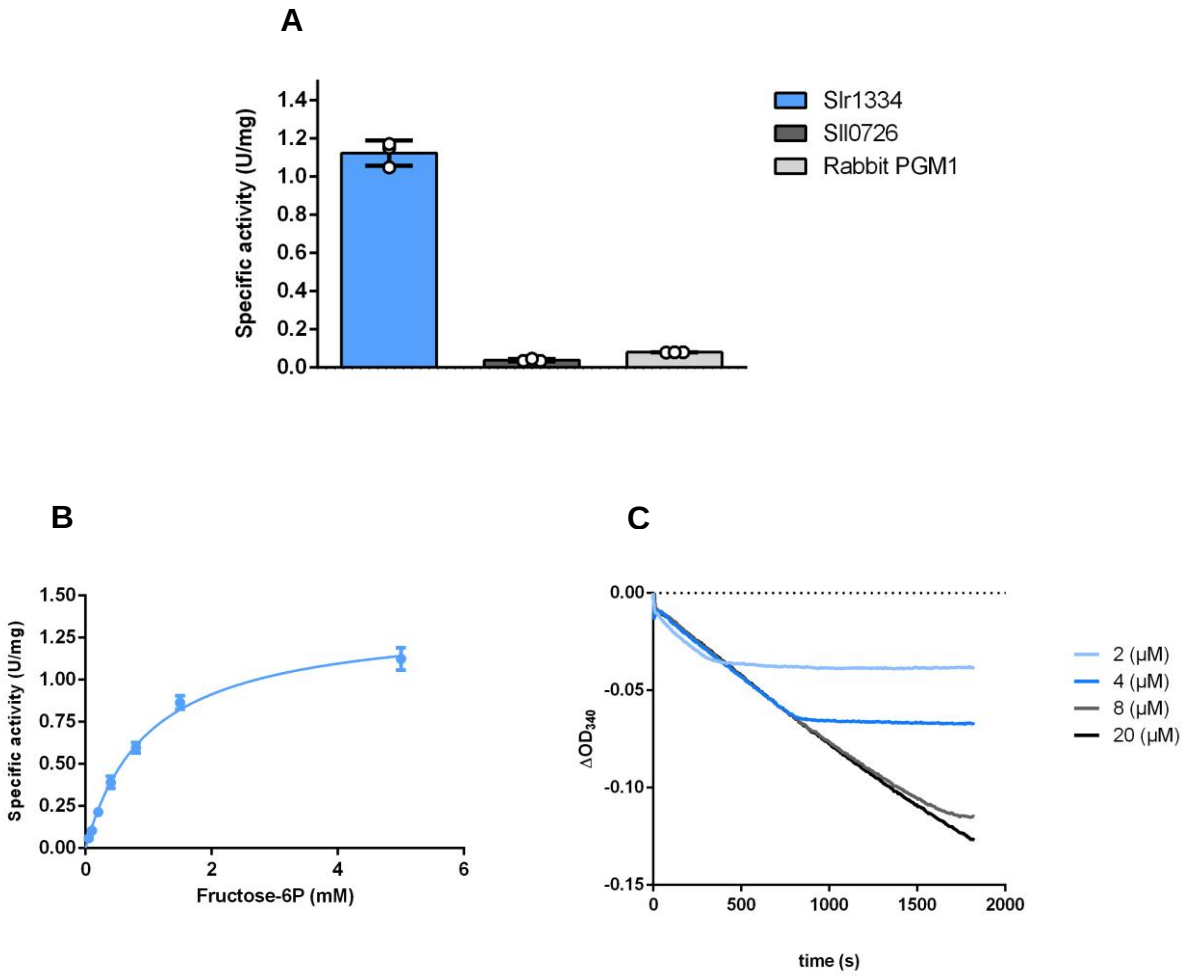

Figure 6: Slr1334 catalyzes the reverse reaction to form Frc-1,6-BP out of Glc-1,6-BP and Frc-6P

(A) Activity of Slr1334 (blue), Sll0726 (grey), and rabbit PGM1 (black) using 50 µM Glc-1,6-BP and 5 mM Frc-6P. (B) Michaelis-Menten kinetics of Slr1334 using different concentrations of Frc-6P and 50 µM Glc-1,6-BP. (C) Slr1334 reaction at different concentrations of Glc-1,6-BP and 5 mM Frc-1P. Three replicates were measured for each datapoint. Error bars represent the SD; asterisks represent the statistical significance.

Substrate	**K_m (mM)**	**k_{cat} (s^{-1})**	**k_{cat}/K_m ($M^{-1}s^{-1}$)**
Glc-1,6-BP	<0.002	1.2 ± 0.03	600000
Frc-6P	1.0 ± 0.07		>1200

Table 3: Kinetic parameters of Frc-1,6-BP synthesis by Slr1334
K_m and Kcat values are means of triplicates with ± SD.

389 **The Glc-1,6-BP synthase reaction is also performed by other members of the cd05800 group**

390 To determine whether the reaction catalyzed by Slr1334 is representative for αPHM enzymes
391 of the cd05800 family, we decided to analyze the corresponding homologue from the human
392 microbiome associated bacterium *Bacteroides salyersiae*. Therefore, we tested formation of
393 Glc-1,6-BP under the same conditions as described above for Slr1334 by incubating the
394 recombinant cd05800 enzyme from *B. salyersiae* with Frc-1,6-BP and Glc-1P or Glc-6P and
395 subsequently adding the supernatant of this reaction to the Sll0726 assay. As a positive control
396 we used the reaction of Slr1334.
397 The addition of the supernatant from the *B. salyersiae* cd05800 PGM increased the velocity of
398 Sll0726 in a comparable manner as the supernatant of the Slr1334 reaction (**Fig. 7**). This
399 indicates that similar amounts of Glc-1,6-BP have been formed in both reactions, hence
400 revealing that *B. salyersiae* cd05800 PGM catalyzes the same reaction as Slr1334.
401
402
403
404
405
406
407
408
409
410
411
412
413
414

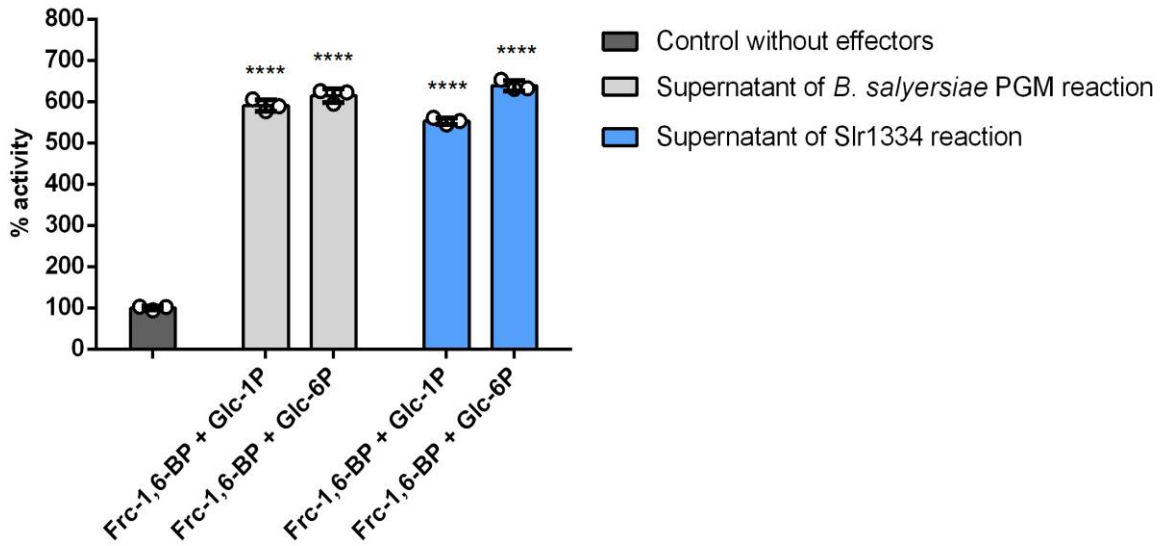

415 **Figure 7: Slr1334 homologue from *B.salyersiae* also forms Glc-1,6-BP out of Frc-1,6-BP**

416 Shown is the activity of Sll0726: blue, after addition of the supernatant of the *B. salyersiae*
417 PGM reaction; in light grey, after addition of the supernatant of the Slr1334 reaction as a
418 positive control; in dark grey, without any effectors as a negative control. The different
419 combinations of substrates used for the *B. salyersiae* PGM and Slr1334 control reaction are
indicated on the X-axis. Values represent relative activity compared to the Sll0726 reaction
without any effectors, which was considered 100%. Error bars represent the SD; asterisks
420 represent the statistical significance.

421 # Discussion

422 Among the key reactions in carbon metabolism are the phosphoryl transfer reactions on
423 different phosphosugars, which are catalyzed by the members of the αPHM superfamily.
424 These reactions are essential for glycogen metabolism, amino sugar metabolism as well as cell
425 wall synthesis and are conserved throughout all domains of life. The interconversion of Glc-1P
426 to Glc-6P and vice versa by PGM is by far the best studied of these reactions and investigation
427 of PGM goes back to the 1940s. It has long been known that PGM requires Glc-1,6-BP as a
428 activator [10]. While in mammals free Glc-1,6-BP has been shown to derive from the reaction of
429 the PGM2L1 enzyme utilizing Glc-1P and 1,3-BPG as substrates, its origin in prokaryotes has
430 remained unknown [3].
431 In this study we used the unicellular cyanobacterium *Synechocystis* sp. PCC6803 as a model
432 organism to identify the first bacterial glucose-1,6-BP synthase. This reversible reaction is a
433 novel function of a member of a distinct αPHM subfamily producing free α-D-Glc-1,6-BP and
434 Frc-6P from Frc-1,6-BP and Glc-1P/Glc-6P.
435 Glc-1,6-BP is essential for PGM activity due to the requirement for phosphorylation of the
436 serine residue at the active site for enzyme activation. The activating reaction converts Glc-
437 1,6-BP into either Glc-1P or Glc-6P. After this initial activation, the interconversion of Glc-1P
438 to Glc-6P is mediated by a transfer of the phosphate group from the serine residue at the
439 active site to the 1' or 6' position of the substrate respectively, forming a Glc-1,6-BP
440 intermediate. This intermediate has to reconfigure inside the enzyme and transfer the
441 phosphate of its 6' or 1' position back to the active site serine leading to the release of Glc-6P
442 or Glc-1P, respectively. As a result of this mechanism, the active site remains phosphorylated
443 and the enzyme is ready for a new cycle. However, it has been shown that the phosphorylation
444 of PGM at the active site is lost after an average of 15-20 reaction cycles by a spontaneous
445 dissociation of the intermediate Glc-1,6-BP leaving behind an inactive dephosphoenzyme.
446 Therefore, a constant level of Glc-1,6-BP is necessary to ensure that PGM is kept in an active
447 state [20, 21]. While the loss of the intermediate might be regarded as an unfavorable event, it
448 can also be considered as a regulatory mechanism that enables regulation of PGM activity
449 based on Glc-1,6-BP levels. For other αPHMs like PMM and PNGM it is known that the
450 corresponding intermediates (e.g. α-D-mannose-1,6-BP and α-D-glucosamine-1,6-BP) are
451 formed during the reaction of the respective enzymes in the same way as for PGM but no

452 source of those intermediates is known that would enable an initial activation of these αPHMs
453 or would keep them in an active state overtime when phosphorylation is lost. However, since
454 many members of the αPHM family show at least some residual PGM activity, Glc-1,6-BP was
455 suggested to be the activating compound for these enzymes as well. This has in fact been
456 shown for PNGM from *E. coli* which is considered to be an essential enzyme [22]. This makes the
457 role of Glc-1,6-BP in carbon metabolism even more relevant and would explain the failed
458 attempts to delete the *slr1334* gene [17].
459 In mammals, it was shown that Glc-1,6-BP can also regulate central enzymes of carbon
460 pathways by inhibiting hexokinases, 6-phosphogluconate dehydrogenase and fructose-1,6-
461 bisphosphatase and by activating phosphofructokinase and pyruvate kinase [12]. Further studies
462 in mammals showed that Glc-1,6-BP is especially elevated in brain tissue to a level that highly
463 exceeds the regulatory concentrations needed for PGM activity, and that reduced levels of
464 Glc-1,6-BP cause severe neurological problems [23]. This indicates that at least in mammals
465 there are likely more functions of Glc-1,6-BP to be discovered. Given the important role of Glc-
466 1,6-BP in eukaryotic metabolism, it is surprising that very little is known on the role of Glc-1,6-
467 BP in bacterial physiology. The only study about the origin of α-D-Glc-1,6-BP production in
468 bacteria proposed a phosphodismutase reaction with Glc-1P as the sole substrate in *E. coli*
469 [24]. Moreover, the levels of Glc-1,6-BP in eukaryotes are affected by a specific Glc-1,6-BP
470 phosphatase, PMM1, which is a phosphomannomutase that is not part of the αPHM
471 superfamily. Whether a homologue exists in bacteria is currently unknown [24].
472 In absence of Glc-1,6-BP, both Slr1334 and Sll0726 showed low PGM activity. This residual
473 activity can be explained by the fact that a phosphorylation of the active site serine can also
474 be achieved at high concentrations of Glc-1P but at a much lower efficiency, leading to high
475 K_m values and overall strongly reduced activity [11]. In the presence of Frc-1,6-BP, Sll0726 was
476 strongly inhibited, which agrees with the inhibitory effect of Frc-1,6-BP on other PGMs [19, 25].
477 By contrast, Frc-1,6-BP enhanced the overall catalytic activity of Slr1334, primarily because of
478 a strongly decreased K_m. This effect can now be attributed to the formation of the activator
479 Glc-1,6-BP.
480 Like mammalian PGM2L1, Slr1334 can utilize 1,3-BPG as a phosphorylating compound for Glc-
481 1,6-BP formation, however with a much lower efficiency than with Frc-1,6-BP. For the
482 mammalian PGM2L1 a reverse reaction (formation of 1,3-BPG and Glc-1P from Glc-1,6-BP and
483 3-PG) has not been shown. For Slr1334, we could clearly show reversibility of the reaction,

484 producing Frc-1,6-BP from Glc-1,6-BP and Frc-6P. Provided that both directions of the reaction
485 have similar kinetic properties, Slr1334 appears to be a *bona-fide* Glc-1,6-BP synthase, which
486 is prone to activate the main PGM Sll0726.
487 In contrast to Glc-1,6-BP, Frc-1,6-BP is an obligatory intermediate in glycolysis,
488 gluconeogenesis and Calvin-Benson-Bassham cycle. In contrast to mammalian PGM2L1,
489 *Synechocystis* Slr1334 uses this sugar as the major substrate for Glc-1,6-BP synthesis. This links
490 the synthesis of Glc-1,6-BP to the levels of Frc-1,6-BP. Its steady state level depends on the
491 activity of the opposing reactions of phosphofructokinase (Pfk) and Fructose-1,6-
492 bisphosphatase (FBPase), both of which are regulated in an opposite manner: While PFK is
493 usually activated by the low energy state metabolites ADP and AMP and downregulated by
494 the high energy state metabolites ATP and citrate, FBPase is downregulated by AMP while
495 unaffected by high energy compounds. The level of Frc-1,6-BP is further determined by the
496 Frc-1,6-BP-aldolase activity. Frc-1,6-BP is also known to be an allosteric activator of pyruvate
497 kinase (PK), the final step in glycolysis [26].
498 Altogether, in the cyanobacterium *Synechocystis* PCC6803, Frc-1,6-BP appears to have two
499 counteracting effects on PGM activity. On the one hand, it acts as a direct inhibitor of PGM;
500 on the other hand, it gives rise to the synthesis of the PGM activator Glc-1,6-BP through the
501 activity of Slr1334. Furthermore, since these double phosphorylated sugars may affect further
502 enzyme reactions, by connecting these two metabolites, Slr1334 might represent a crucial
503 regulatory point in glycolysis (**Fig. 8**). This conclusion would further underline the essential
504 role of *slr1334* [17].
505 Interestingly, our phylogenetic analysis revealed the cd05800 subfamily as the most
506 primordial group of phosphoglucomutases. This group appears to be especially present in
507 bacterial classes that are considered deeply branching bacteria meaning they are relatively
508 close to the last common universal ancestor (LUCA). Examples for this are the classes of
509 Deinococci, Aquificae, Thermotogae, Bacteroidetes and Cyanobacteria, where this PGM
510 subfamily is widely distributed. This finding is supported by the fact that cd05800 members
511 can also be found in archaea. In agreement with this, the first characterized representative of
512 this group, Slr1334 shows both PGM and Glc-1,6-BP activity. This suggests that in primordial
513 systems these PGMs with broad functionality could have performed PGM reactions without
514 the requirement for specific Glc-1,6-BP synthase enzymes. During subsequent functional
515 diversification, the PGMs may have adopted unique functions, with specialization towards

516 efficient conversion of Glc-6-P into Glc-1P on the one hand, and more specialized formation
517 of the activating compound Glc-1,6-BP on the other hand. This assumption agrees with the
518 observation that many bacteria that have a cd05800 family member also possess a specialized
519 PGM of the cd05801 or cd03085 subfamily for efficient Glc-6P – Glc-1P conversion. This
520 includes the ensemble of all cyanobacteria. Conversely, many pathogenic bacteria that have
521 a PGM of the cd03089 type lack a cd5800 representative (**Table S4**) which raises the question
522 how those strains produce Glc-1,6-BP. To clarify these issues further investigations on αPHM
523 members from various bacterial groups are required.
524 We were able to show that the cd05800 PGM from the human gut commensal bacterium *B.*
525 *salyersiae* also catalyzes the synthesis of Glc-1,6-BP out of Frc-1,6-BP like Slr1334 (**Fig. 7**). In
526 the case of *B. salyersiae*, the enzyme appears to have an even higher catalytic efficiency for
527 the Glc-1,6-BP synthase reaction than for the standard PGM reaction (**Fig. S1**). Therefore, we
528 conclude that the formation of Glc-1,6-BP is a general feature of this group of PGMs.
529 Interestingly, members of the cd05800 group are also present in emerging human pathogenic
530 species like *Vibrio, Eggerthella* and *Brachyospyra* (**Fig. 1**) and are likely to play a key role in the
531 metabolism of these pathogens. In fact, due to their crucial role in capsule and cell wall
532 synthesis PGMs have been suggested as novel targets for the development of antiinfectives in
533 prophylactic and therapeutic interventions [5, 27]. It is tempting to speculate that Glc-1,6-BP
534 synthases of the cd05800 family, in virtue of their absence in eukaryotes, may also be
535 interesting candidates for the development of novel drugs modulating the microbiota with
536 little collateral damage to the host.
537
538
539
540
541
542
543
544
545
546
547

548 # Methods

549 **Isothermal, Single-Reaction DNA Assembly (Gibson Cloning)**

550 Cloning was performed as described by Gibson, Young [28] using *E. coli* NEB10β cells (details in
551 **Table S5**). All primers and plasmids used are shown in **Table S3** and **Table S4**, respectively.
552

553 **Cultivation of *Escherichia coli***

554 If not otherwise stated *E. coli* was grown in Luria-Bertani medium at 37°C [29]. For growth on
555 plates, 1.5% (w/v) agar-agar was added. For cells containing plasmids, the appropriate
556 concentration of antibiotics was used. All *E. coli* strains used in this study are listed in **Table**
557 **S5.**
558

559 **Protein overexpression and purification**

560 The plasmids used for protein overexpression are shown in **Table S4.** *Escherichia coli* Rosetta-
561 gami (DE3) (details **Table S5**) was used for the overexpression of all proteins. For this, cells
562 were cultivated in 2xYT (3.5% tryptone, 2% yeast extract, 0.5% NaCl; 1L of culture in 5L flasks)
563 at 37 °C until reaching exponential growth (OD_{600} 0.6-0.8). Protein overexpression was
564 induced by adding 75 µg/L anhydrotetracycline, followed by incubation at 20°C for 16 h. Cells
565 were harvested by centrifugation at 4000 g for 10 min at 4 °C. Cell disruption was performed
566 by sonication in 40 mL of lysis buffer (100 mM Tris-HCl pH 7.5, 500 mM NaCl, 10 mM $MgCl_2$,
567 20 mM Imidazole for His-tagged proteins and 100 mM Tris-HCl pH 8, 150 mM NaCl, 10 mM
568 $MgCl_2$ for Strep-tagged proteins) Lysis buffers were supplemented with DNAse I, and
569 cOmplete™ protease inhibitor cocktail (Roche, Basel)). The cell lysate was centrifuged at
570 40,000 g for 45 min at 4°C and the supernatant was filtered with a 0.22 µM filter.
571 For the purification of His-tagged proteins, 5 mL Ni-NTA HisTrap columns (GE Healthcare,
572 Illinois, USA) were used. The cell extracts were loaded onto the columns, washed with wash
573 buffer (50 mM Tris-HCl pH 7.4, 500 mM NaCl, and 50 mM Imidazole) and eluted with elution
574 buffer (50 mM Tris-HCl pH 7.4, 500 mm NaCl, and 500 mM Imidazole).
575
576
577

578 **Measurement of PGM activity of Sll0726 and Slr1334 in vitro**

579 Buffer for enzymatic reactions was composed of 50 mM HEPES-KOH pH 7.5, 150 mM KCl, 10
580 mM $MgCl_2$, 1 mM $NADP^+$, 1 mM DTT and 1 U/mL G6PDH from *Saccharomyces cerevisiae*
581 (G6378, Sigma Aldrich). For Sll0726 activity, 60 ng of Strep-tagged purified protein was added
582 to each reaction. For slr1334 activity, 650 ng of purified protein was added. For tests with
583 saturating Glc-1,6-BP concentrations, 60 µM Glc-1,6-BP have been used. Reaction was started
584 by the addition of glucose-1P. Reactions were carried out in a total of 300 µl in a 96-well
585 microplate. Absorption change at 340 nm was continuously measured for 15 min at 30 °C in a
586 TECAN Spark® Multiplate reader (Tecan Group AG, Männedorf, Switzerland). At least three
587 replicates were measured.
588

589 **Measurement of Glc-1,6-BP formation**

590 The reaction buffer was composed of 50 mM HEPES-KOH pH 7.5, 150 mM KCl and 10 mM
591 $MgCl_2$. To test the formation of Glc-1,6-BP out of Frc-1,6-BP 1 mM Frc-1,6-BP, 1 mM Glc1P or
592 1 mM Glc-6P were added in different combinations. To test the formation of Glc-1,6-BP out of
593 1,3-BPG instead of Frc-1,6-BP, 1 mM of ATP, 1 mM 3-PG and 60 µg PGK have been used.
594 Sll0726 and Slr1334 concentration were 30 µg/ml. The reactions were performed for 1.5 h at
595 30 °C followed by heat inactivation at 90°C for 10 minutes with subsequent centrifugation at
596 25000 g for 10 minutes at 4° C. The supernatants of the various reactions were used at 1:10
597 dilution in the Sll0726 activity assay.
598

599 **Frc-1,6-BP aldolase assay**

600 To measure the formation of Frc-1,6-BP by Slr1334, the reaction buffer was composed of 50
601 mM HEPES-KOH pH 7.5, 150 mM KCl, 10 mM $MgCl_2$, 0.2 mM NAD, 7 µg Slr1334, 1U/ml aldolase
602 from rabbit muscle and 1U/ml GDH from rabbit muscle. Concentrations of Glc-1,6-BP and Frc-
603 6P were varying depending on the experiment. Reaction was started by the addition of Glc-
604 1,6-BP or Frc-6P depending on the experiment.
605 To measure residual Frc-1,6-BP after running the Slr1334 reaction, the buffer was composed
606 of 50 mM HEPES-KOH pH 7.5, 150 mM KCl, 10 mM $MgCl_2$, 0.2 mM NAD, 0.02U/ml aldolase
607 from rabbit muscle and 1U/ml GDH from rabbit muscle.
608 All reactions were carried out in a total of 300 µl in a 96-well microplate Absorption change at
609 340 nm was continuously measured for 15 min at 30 °C in a TECAN Spark® Multiplate reader

610 (Tecan Group AG, Männedorf, Switzerland). The enzymatic activity was then calculated. At
611 least three replicates were measured.
612
613 **LC-MS measurement**

614 Sample preparation:
615 Reaction buffer was composed of 50 mM HEPES-KOH pH 7.5, 150 mM KCl and 10 mM $MgCl_2$.
616 For the reaction without enzyme 500 µM Frc-1,6-BP and 1 mM Glc1-P were added. For the
617 Slr1334 reaction 30 µg of Slr1334 have been used additionally. Reaction was carried out in a
618 total volume of 1 ml at 30 °C for 1h. Afterwards reaction was stopped by heat inactivation at
619 90° C followed by centrifugation at 25000 g for 10 minutes at 4°C.
620 For degradation of Frc-1,6-BP 1 mM NADH, 2U/ml of aldolase from rabbit muscle and 2U/ml
621 of GDH from rabbit muscle were added. Reaction was carried out followed by inactivation at
622 the same conditions as before.
623 LC/MS analysis:
624 LC/MS analysis was performed using an electrospray ionization time of flight (ESI-TOF) mass
625 spectrometer (MicrOTOF II; Bruker Daltonics), operated in negative ion-mode connected to
626 an UltiMate 3000 high-performance liquid chromatography (HPLC) system (Dionex). The
627 separation in the HPLC was carried out using a SeQuant ZIC-pHILIC column (PEEK 150 × 2.1
628 mm, 5 µm, 110 Å, Merck) at 30°C with an CH_3CN (buffer A) and 100 mM $(NH_4)_2CO_3$, pH 9
629 (buffer B) buffer system. A single run (injection volume of 5 µl) was performed with a flow rate
630 of 0.2 ml/min and a linear gradient of 25 min, reducing the concentration of buffer A from 82
631 to 42 %. Before (5 min) and after (10 min) the gradient, the column was equilibrated with 82 %
632 buffer A.
633
634 **Phylogenetic analysis of αPHM subfamilies**

635 The occurrence of members of the αPHM subfamilies was investigated in organisms included
636 in the NCBI RefSeq_protein database. Phylogenetic tree data were created using the ClustalW
637 implementation from the European Bioinformatics Institute (EMBL-EBI) and the phylogenetic
638 tree was created using the Interactive Tree Of Life (iTOL) v5 online tool [30, 31].
639
640

641 **Statistical analysis**

642 Statistical details for each experiment can be found in the figure legends. GraphPad PRISM
643 was used to perform one-sided ANOVA to determine the statistical significance. Asterisks (*)
644 in the figures symbolize the p-value: One asterisk represents $p \leq 0.05$, two asterisks $p \leq 0.01$,
645 three asterisks $p \leq 0.001$, and four asterisks $p \leq 0.0001$

646

647 # References

648

649 1. Shackelford, G.S., C.A. Regni, and L.J. Beamer, *Evolutionary trace analysis of the α-D-*
650 *phosphohexomutase superfamily.* Protein Science, 2004. **13**(8): p. 2130-2138.

651 2. Stiers, K.M., A.G. Muenks, and L.J. Beamer, *Biology, Mechanism, and Structure of*
652 *Enzymes in the α-d-Phosphohexomutase Superfamily.* Advances in protein chemistry
653 and structural biology, 2017. **109**: p. 265-304.

654 3. Maliekal, P., et al., *Molecular identification of mammalian phosphopentomutase and*
655 *glucose-1,6-bisphosphate synthase, two members of the alpha-D-*
656 *phosphohexomutase family.* J Biol Chem, 2007. **282**(44): p. 31844-51.

657 4. Lu, S., et al., *CDD/SPARCLE: the conserved domain database in 2020.* Nucleic Acids
658 Res, 2020. **48**(D1): p. D265-d268.

659 5. Regni, C., P.A. Tipton, and L.J. Beamer, *Crystal structure of PMM/PGM: an enzyme in*
660 *the biosynthetic pathway of P. aeruginosa virulence factors.* Structure, 2002. **10**(2): p.
661 269-79.

662 6. Regni, C., et al., *Structural basis of diverse substrate recognition by the enzyme*
663 *PMM/PGM from P. aeruginosa.* Structure, 2004. **12**(1): p. 55-63.

664 7. Akutsu, J.-i., et al., *Characterization of a Thermostable Enzyme with*
665 *Phosphomannomutase/Phosphoglucomutase Activities from the Hyperthermophilic*
666 *Archaeon Pyrococcus horikoshii OT3.* The Journal of Biochemistry, 2005. **138**(2): p.
667 159-166.

668 8. Liu, Y., W.J. Ray, Jr., and S. Baranidharan, *Structure of rabbit muscle*
669 *phosphoglucomutase refined at 2.4 A resolution.* Acta Crystallogr D Biol Crystallogr,
670 1997. **53**(Pt 4): p. 392-405.

671 9. Backe, P.H., et al., *Structural basis for substrate and product recognition in human*
672 *phosphoglucomutase-1 (PGM1) isoform 2, a member of the α-d-phosphohexomutase*
673 *superfamily.* Scientific Reports, 2020. **10**(1): p. 5656.

674 10. Leloir, L.F., R.E. Trucco, and et al., *The co-enzyme of phosphoglucomutase.* Arch
675 Biochem, 1948. **19**(2): p. 339.

676 11. Naught, L.E. and P.A. Tipton, *Kinetic Mechanism and pH Dependence of the Kinetic*
677 *Parameters of Pseudomonas aeruginosa*
678 *Phosphomannomutase/Phosphoglucomutase.* Archives of Biochemistry and
679 Biophysics, 2001. **396**(1): p. 111-118.

680 12. Carreras, J., et al., *Bisphosphorylated metabolites of glycerate, glucose, and fructose:*
681 *Functions, metabolism and molecular pathology.* Clinical Biochemistry, 1986. **19**(6): p.
682 348-358.

13. Joshi, J.G. and P. Handler, *PHOSPHOGLUCOMUTASE. I. PURIFICATION AND PROPERTIES OF PHOSPHOGLUCOMUTASE FROM ESCHERICHIA COLI.* J Biol Chem, 1964. **239**: p. 2741-51.

14. Lindahl, M. and F.J. Florencio, *Thioredoxin-linked processes in cyanobacteria are as numerous as in chloroplasts, but targets are different.* Proceedings of the National Academy of Sciences, 2003. **100**(26): p. 16107-16112.

15. Mehra-Chaudhary, R., et al., *Crystal structure of a bacterial phosphoglucomutase, an enzyme involved in the virulence of multiple human pathogens.* Proteins, 2011. **79**(4): p. 1215-1229.

16. Doello, S., et al., *Regulatory phosphorylation site tunes Phosphoglucomutase 1 as a metabolic valve to control mobilization of glycogen stores.* bioRxiv, 2021: p. 2021.04.15.439997.

17. Lian Liu, H.H., Hong Gao, and Xudong Xu, *Role of two phosphohexomutase genes in glycogen synthesis in Synechocystis sp. PCC6803.* Chinese Science Bulletin, 2013. **58**(36).

18. Maino, V.C. and F.E. Young, *Regulation of Glucosylation of Teichoic Acid: II. PARTIAL CHARACTERIZATION OF PHOSPHOGLUCOMUTASE IN BACILLUS SUBTILIS 168.* Journal of Biological Chemistry, 1974. **249**(16): p. 5176-5181.

19. Fazi, A., et al., *Purification and partial characterization of the phosphoglucomutase isozymes from human placenta.* Prep Biochem, 1990. **20**(3-4): p. 219-40.

20. Naught, L.E. and P.A. Tipton, *Formation and reorientation of glucose 1,6-bisphosphate in the PMM/PGM reaction: transient-state kinetic studies.* Biochemistry, 2005. **44**(18): p. 6831-6.

21. Ray, W.J., Jr. and G.A. Roscelli, *A KINETIC STUDY OF THE PHOSPHOGLUCOMUTASE PATHWAY.* J Biol Chem, 1964. **239**: p. 1228-36.

22. Jolly, L., et al., *Autophosphorylation of Phosphoglucosamine Mutase from Escherichia coli.* Journal of Bacteriology, 2000. **182**(5): p. 1280-1285.

23. Morava, E., et al., *Impaired glucose-1,6-biphosphate production due to bi-allelic PGM2L1 mutations is associated with a neurodevelopmental disorder.* Am J Hum Genet, 2021. **108**(6): p. 1151-1160.

24. Veiga-da-Cunha, M., et al., *Mammalian phosphomannomutase PMM1 is the brain IMP-sensitive glucose-1,6-bisphosphatase.* The Journal of biological chemistry, 2008. **283**(49): p. 33988-33993.

25. Maino, V.C. and F.E. Young, *Regulation of glucosylation of teichoic acid. II. Partial characterization of phosphoglucomutase in Bacillus subtilis 168.* J Biol Chem, 1974. **249**(16): p. 5176-81.

26. Waygood, E.B., J.S. Mort, and B.D. Sanwal, *The control of pyruvate kinase of Escherichia coli. Binding of substrate and allosteric effectors to the enzyme activated by fructose 1,6-bisphosphate.* Biochemistry, 1976. **15**(2): p. 277-282.

27. Zhang, Y., et al., *The Brucella melitensis M5-90 phosphoglucomutase (PGM) mutant is attenuated and confers protection against wild-type challenge in BALB/c mice.* World Journal of Microbiology and Biotechnology, 2016. **32**(4): p. 58.

28. Gibson, D.G., et al., *Enzymatic assembly of DNA molecules up to several hundred kilobases.* Nature Methods, 2009. **6**(5): p. 343-345.

29. Bertani, G., *Studies on lysogenesis. I. The mode of phage liberation by lysogenic Escherichia coli.* J Bacteriol, 1951. **62**(3): p. 293-300.

30. Letunic, I. and P. Bork, *Interactive Tree Of Life (iTOL) v5: an online tool for phylogenetic tree display and annotation.* Nucleic Acids Research, 2021. **49**(W1): p. W293-W296.

31. Madeira, F., et al., *The EMBL-EBI search and sequence analysis tools APIs in 2019.* Nucleic acids research, 2019. **47**(W1): p. W636-W641.

Acknowledgements

We thank Libera Lo Presti for her assistance in writing this manuscript and Gaia Bianchi for support in performing enzymatic assays.

This work was supported by FOR2816 “The Autotrophy-Heterotrophy Switch in Cyanobacteria: Coherent Decision-Making at Multiple Regulatory Layers” and EXC2121 “Controlling Microbes to Fight Infections (CMFI).

Author contributions

N.N. performed cloning, protein purification, enzymatic assays phylogenetic analysis and wrote manuscript. S.F. performed LC/MS analysis. K.F. conceived study, interpreted data and edited manuscript.

Competing interests

The authors declare no competing interest.

766 # Figure Legends

767

768 **Figure 1**: **Phylogenetic tree of the αPHM subfamilies that are considered to be "PGM-like"**
769 **according to CDD**
770
771 The tree was built on the taxonomy based on the protein sequences present in the NCBI
772 RefSeq_protein database. The CDD subfamilies cd03086, cd03088, cd05802 and cd05805,
773 which are known to catalyze distinct reactions, were omitted from the analysis. The organisms
774 investigated in this study are highlighted in bold letters.
775

776 **Figure 2: Slr1334 shows lower PGM activity then Sll0726 and behaves differently in presence**
777 **of Frc-1,6-BP**

778 Shown are the Michaelis-Menten kinetics of Sll0726 (A) and Slr1334 (B): in black, without
779 addition of effectors; in light grey in the presence of 60 µM Glc-1,6-BP; in blue, in the presence
780 of 100 µM Frc-1,6-BP. Three replicates were measured for each data-point. Error bars
781 represent the SD.

782

783 **Figure 3: Slr1334 produces a compound out of Frc-1,6-BP that strongly activates Sll0726**

784 Shown is the Sll0726 activity: in dark grey, at different Glc-1,6-BP concentrations; in blue, after
785 addition of the supernatant of the Slr1334 reaction; in light grey, after addition of the
786 supernatant of the Sll0726 reaction as a control; in white, after addition of the sole
787 phosphosugars without enzyme as further control. The different combinations of substrates
788 used for the Slr1334 reaction and controls are indicated on the X-axis. Values represent
789 relative activity compared to the Sll0726 reaction with 0 µM Glc-1,6-BP, which was considered
790 100%. Three biological replicates were measured for each datapoint. Error bars represent the
791 SD; asterisks represent the statistical significance

792

793 **Figure 4: LC-MS analysis reveals that Slr1334 metabolizes Frc-1,6-BP into a molecule of**
794 **identical mass that is not degraded by Frc-1,6-BP-aldolase**

795 Analysis of the products of the reaction without (A) and with Slr1334 (B) via LC/MS. Shown are
796 the base peak chromatograms (BPC) in the mass range $(M-H)^-$ m/z = 79–1,601 (grey) and the
797 extracted ion chromatograms (EIC) based on the exact masses of NAD+ $(M-H)^-$= 662.102 m/z
798 (light blue), NADH $(M-H)^-$= 664.118 m/z (red), Glycerol 3-P $(M-H)^-$= 171.006 m/z (yellow), Glc-
799 1,6-BP/Frc-1,6-BP $(M-H)^-$= 338.989 m/z (purple). The presence of the NAD+ (blue) and
800 Glycerol-3P (yellow) peaks in (B) shows that Frc-1,6-BP was not fully metabolized into Glc-1,6-
801 BP. Magnification and adjustment of the graphs in (A) and (B) is clear evidence of the absence
802 (**C**) or formation (**D**) of Glc-1,6-BP.

803
804
805
806
807

808 **Figure 5: Slr1334 produces Glc-1,6-BP out of Frc-1,6-BP in an equilibrium reaction**

809 Shown is the Frc-1,6-BP-aldolase activity: in dark blue, after addition of the supernatant of
810 the Slr1334 reaction; in light blue, after addition of the supernatant of the Sll0726 reaction as
811 a control; in black, after addition of the supernatant without any enzyme. In dark grey and
812 light grey, the aldolase activity measured at Frc-1,6-BP concentrations of 25 µM and 50 µM,
813 respectively, as further control.
814 Frc-1,6-BP was used at concentrations of 500 µM in the Slr1334 reaction and respective
815 control reactions. Therefore, its final concentration in the Sll0726 assay after 1:10 dilution was
816 expected to be 50 µM assuming no consumption of Frc-1,6-BP in the Slr1334 reaction. Three
817 replicates were measured for each datapoint. Error bars represent the SD.
818

819 **Figure 6: Slr1334 catalyzes the reverse reaction to form Frc-1,6-BP out of Glc-1,6-BP and Frc-**
820 **6P**

821 (A) Activity of Slr1334 (blue), Sll0726 (grey), and rabbit PGM1 (black) using 50 µM Glc-1,6-BP
822 and 5 mM Frc-6P. (B) Michaelis-Menten kinetics of Slr1334 using different concentrations of
823 Frc-6P and 50 µM Glc-1,6-BP. (C) Slr1334 reaction at different concentrations of Glc-1,6-BP
824 and 5 mM Frc-1P. Three replicates were measured for each datapoint. Error bars represent
825 the SD; asterisks represent the statistical significance.
826

827 **Figure 7: Slr1334 homologue from *B.salyersiae* also forms Glc-1,6-BP out of Frc-1,6-BP**

828 Shown is the activity of Sll0726: blue, after addition of the supernatant of the *B. salyersiae*
829 PGM reaction; in light grey, after addition of the supernatant of the Slr1334 reaction as a
830 positive control; in dark grey, without any effectors as a negative control. The different
831 combinations of substrates used for the *B. salyersiae* PGM and Slr1334 control reaction are
832 indicated on the X-axis. Values represent relative activity compared to the Sll0726 reaction
833 without any effectors, which was considered 100%. Error bars represent the SD; asterisks
834 represent the statistical significance.

835

836 **Figure 8: Potential role of Slr1334 in glycolysis**

837 Shown is the potential role of Slr1334 in regulating activity of αPHMs and the concentration
838 of key metabolites in glycolysis. PGM: Phosphoglucomutase; PGI: Glc-6P-Isomerase; PFK:
839 Phosphofruktokinase; FBAse: Fructose-6P phosphatase; FBA: Frc-1,6-BP-aldolase; TPI:
840 Triosephosphate isomerase; GAPDH: Glyceraldehyde-3P dehydrogenase; DHAP:
841 Dihydroxyacetone phosphate
842